Understanding salt or PEG induced attractive interactions to crystallize biological macromolecules

Annette Tardieu[a*], Françoise Bonneté[b], Stéphanie Finet[c] and Denis Vivarès[b]

[a]LMCP, Case 115, 4 Place Jussieu, F75252 Paris Cedex 05, France, [b]CRMC2 – CNRS, Campus de Luminy, case 913, F-13288 Marseille Cedex 09, France and [c]ESRF, BP220, F38043 Grenoble Cedex, France. E-mail: Annette.Tardieu@lmcp.jussieu.fr

Phase diagrams of biological macromolecules are governed by an appropriate combination of interaction potentials in solution. Repulsive regimes favor solubility, whereas the presence of attractive potentials may induce a variety of phase transitions, including the desired macromolecular crystallization. The forces at work may be analyzed with a combination of small angle X-ray scattering and of numerical treatments. From the results obtained with a variety of model systems, the respective advantages and drawbacks of using monovalent salts or PEGs as crystallizing agents are discussed.

Keywords: proteins; polyethylene glycol; interactions; phase diagrams; crystallization; small angle X-ray scattering

1. Introduction

It is common practice in the colloid field to calculate phase diagrams from the interaction potentials in solution, and it is well known that the shapes of the phase diagrams, the presence of stable or metastable phase separations or phase transitions are determined by the ratio of the attraction range and of the macromolecular diameter (e.g. Hansen & McDonald, 1986, Vliegenthart & Lekkerkerker, 2000). Following the track, biological macromolecules were thoroughly investigated by many groups. The good news are that there is a logic behind biomacromolecular crystallization, i.e. *increasing or decreasing solubility is in general equivalent to increase or decrease repulsive interactions and crystallization occurs in attractive regimes or close to* (George & Wilson 1994, Muschol & Rosenberger 1995, Ducruix *et al*., 1996, Velev *et al*., 1998, Hitscherich *et al*., 2000, Yau *et al*., 2000, Vivarès & Bonneté 2002). Our contribution was to develop a combination of small angle X-ray scattering (SAXS) and of numerical simulations to analyze the forces at work in biomacromolecular solutions (Vérétout *et al*., 1989, Tardieu *et al*., 1999). Ideally, the phase diagrams would then be calculated from the interactions and therefore the conditions to choose to have a chance to get crystals (e.g. Haas *et al*., 1999). The question that we address in this paper is, what do we know now and what is missing ?

2. Materials and methods

2.1. SAXS and virial coefficients

SAXS can be used to measure virial coefficients and is the best technique to provide us with the interaction potentials. To make a long story short (Vérétout *et al.*, 1989; Tardieu *et al.*, 1999) the X-ray scattering curves, I(c,s), where s is the scattering vector ($s = 2\sin\theta/\lambda$) and c, (g/cm^3), the macromolecular concentration, obtained with monodisperse solutions of globular macromolecules, may be written as the product of the form factor, I(0,s), (scattered intensity of one particle), by the structure factor, S(c,s), which depends upon the particle distribution*:*

$$I(c,s) = I(0,s) \cdot S(c,s) \qquad [1]$$

The form factor (recorded at low concentration) gives information on the shape and the oligomeric state of the particles. Guinier plots i.e. plots of Log I(c,s) as a function of s^2, allow us to extrapolate the curves to the origin and therefore to determine I(0,0) and S(c,0) as a function of c. The variation of the structure factor as a function of the particle concentration readily indicates the type of interactions, repulsive and attractive, present in solution. With repulsive interactions, the particles are evenly distributed and S(c,0) is lower than 1. With attractive interactions, fluctuations in the particle distribution are observed and S(c,0) is larger than 1 (note, however, that the extrapolation is only possible with attractive interactions or weak repulsive ones (Bonneté *et al*., 1997)).

The second virial coefficients, A_2 (mol ml g^{-2}), can then be determined from concentration series according to (Bonneté *et al*., 1999):

$$1/S(c,0) = 1 + 2\,MA_2c \qquad [2]$$

The second virial coefficient is itself defined from the osmotic pressure, Π, of the macromolecular solution**:**

$$\Pi/cRT = 1/M + A_2c + A_2c^2 + \ldots \qquad [3]$$

where T is the absolute temperature, R the gas constant, 8.31 J mol^{-1} K^{-1}.

2.2. SAXS, numerical simulations and potential shapes

Interaction potentials usually have repulsive and attractive components. In the numerical simulations (Belloni, 1988), the total potential is considered as made of two components, one repulsive and one attractive (each one being the sum of all the repulsive / attractive parts respectively). Each component takes the mathematical form of a Yukawa potential, described by three parameters, hard sphere diameter, σ, depth (strength), J, and range, d, according to:

$$u(r)/k_BT = J\,(\sigma/r)\exp[-(r-\sigma)/d] \qquad [4]$$

The structure factors are calculated using statistical mechanical models based on the Ornstein-Zernicke and HNC integral equations (Belloni, 1988). S(c,s) is related to the pair distribution function g(r) by Fourier transformation:

$$S(c,s) = 1 + \rho\int 4\pi^2(g(r)-1)(\sin 2\pi rs/2\pi rs)dr \qquad [5]$$

where $\rho = cN_a/M$ is the number density of particles and M the macromolecular molecular weight (Da).

Therefore, when series of experiments are performed as a function of the crystallizing parameters and as a function of protein concentration, the comparison of experimental structure factors and of calculated ones allows us to determine the best fit parameters of both the repulsive and the attractive components of the interaction potential as described in Tardieu *et al.*, 1999. With all the systems studied so far, such a combination of repulsion and attraction was found sufficient to account for the experimental data. The physical meaning, however, of the interactions experimentally observed may sometimes be difficult to assess.

The second virial coefficient is related to the macromolecular interaction potential, u(r), through**:**

$$A_2 = 2\pi\,N_a/M^2\int(1-\exp(-u(r)/k_BT))r^2\,dr \qquad [6]$$

where N_a is the Avogadro's number and k_B the Boltzman constant. Therefore, A_2 is positive with repulsive interactions and negative with attractive ones. Note that Bonneté & Vivarès, 2002, propose to use a normalized value of A_2.

3. Results

3.1. The DLVO potential as a starting point

Crystallization of biological macromolecules is usually discussed in reference to the position of a "solubility curve" in a phase diagram. A classical phase diagram is given in figure 1a. Below the curve, the macromolecules are soluble in an undersaturated solution. Above, crystal growth may take place. Our interest was to analyze the interactions behind.

Experiments performed on a variety of systems have now shown that the DLVO (from Derjaguin, Landau, Verwey, Overbeek) potential model is usually a good model at low ionic strength (i.e. < 0.2 M ionic strength) for soluble proteins (Verwey & Overbeek 1948), which means that, experimentally, the macromolecules behave as a function of pH and ionic strength as expected with such a potential. The model includes hard sphere, van der Waals and coulombic interactions. Hard sphere interactions mean that two particles cannot interpenetrate, the interaction energy is infinite on contact and zero elsewhere. With small compact proteins, the van der Waals forces were shown to be equivalent to a short range, about 3Å, attractive Yukawa potential of 2-3 k_BT (Malfois *et al*., 1996, Tardieu *et al*., 1999). With proteins in aqueous solvents, electrostatic interactions are always present. In the DLVO model, only direct coulombic interactions are considered.

With monodisperse solutions of identical particles, the average charge is the same whatever the particle and the coulombic interactions, which vary with pH, are repulsive, except at the pI where they cancel. Therefore, except possibly at pI, the van der Waals forces are weaker than the coulombic interactions, which means that *the forces at work, well described by the DLVO potential, will be usually unable to provide the attraction necessary for macromolecular crystallization.* Fortunately, we have at hand two main types of crystallizing agents that can render the interactions more attractive: salt and PEG.

3.2. Salt-induced crystallization: the Hofmeister effect

Salt is known for a long time to act as a crystallizing agent (Arakawa & Timasheff 1985). A number of phase diagrams have been measured, e.g. by the group of Ducruix. They showed that the solubility varies with the type of monovalent salt, following the direct/reverse order of the Hofmeister series (Hofmeister 1888) according to whether the particles are studied at a pH higher/lower than the pI, respectively (Riès-Kautt & Ducruix 1989, Carbonnaux *et al*., 1995).

The effect of monovalent salts on the protein *interactions in solution* has now been analyzed (Muschol & Rosenberger 1995, Tardieu *et al*., 1999). Whatever the particle size, monovalent anions were observed, at medium ionic strength (> 0.2 M), not only to screen the charges, but to induce an additional attraction, specific of the salt type. The attraction is short range, about 3Å, and increases with decreasing temperature (Tardieu *et al*., 1999, Bonneté *et al*., 1999) as illustrated in figure 1b-c. The attraction also follows the direct (or reverse) order of the Hofmeister series according to whether the particles are studied at a pH higher (or lower) than the pI. Monovalent cations do not display such a strong differential effect on the protein interactions. At higher ionic strength, however, a variety of effects may be observed, phase separation, precipitation, or even a return to less attractive conditions, that are not yet fully understood (Boyer *et al*., 1999, Petsev & Vekilov 2000, Costenaro *et al*., 2001). Moreover the case of divalent and trivalent ions (either anions or cations) requires further investigation.

The Hofmeister effect is sufficient to induce an attractive regime and crystallization with small compact proteins (and is probably at

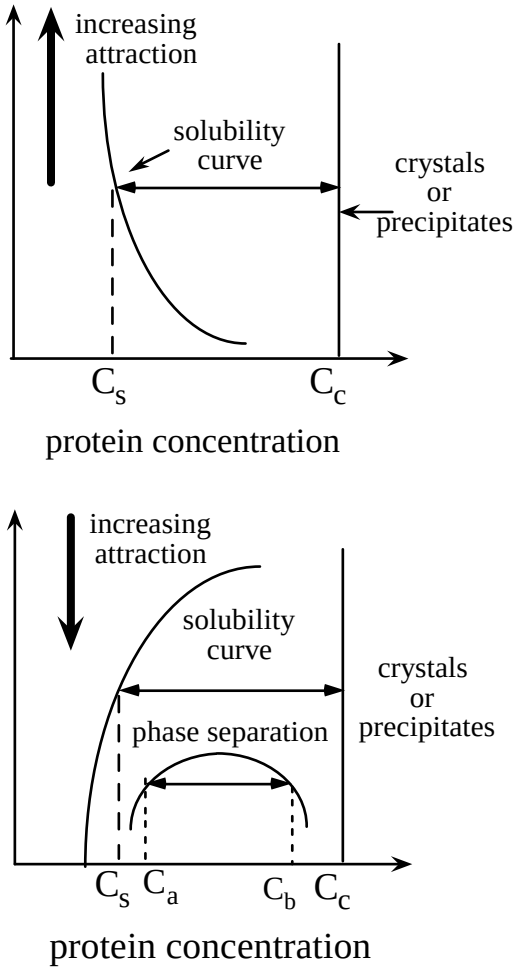

Figure 1
Schematic representation of phase diagrams and potentials. a) Classical representation of the solubility curve. In such a diagram, the underlying protein-protein attraction increases with the concentration of the crystallizing parameter. b) Typical phase diagram observed when the attraction is short range (~3Å) and c) shape of the corresponding potential in the case of lysozyme for a constant value of A_2 (Bonneté et al., 1999). Note the attraction at contact and the repulsion at longer distances. With colloids, the opposite is observed (so-called Lennard-Jones potential).

the origin of the efficiency of ammonium sulfate to crystallize proteins). Typical phase diagrams which correspond to crystallization driven either by the van der Waals attraction or by the Hofmeister effect, i.e. in both cases by short range (about 3 Å), sensitive to temperature attractions, are schematically represented in figure 1b as a function of temperature for a given value of the crystallizing agent. The typical feature of such phase diagrams is that a fluid-fluid phase separation is observed in addition to crystallization, which is metastable with respect to the crystal. The shape of the fluid-fluid phase separation curve is quite well described from the short range attractive potential (Lomakin *et al.*, 1996, Malfois *et al.*, 1996) whereas the position and shape of the solubility curve can be derived from the second virial coefficient (Haas *et al.*, 1999).

Two major problems limit, however, our ability to predict salt induced crystallization. The first one is that *no simple theory has been able so far to account for the Hofmeister effect*. As a consequence, we do not know how to calculate/estimate, the importance of the Hofmeister effect from the solution composition.

The second one is that, with increasing molecular weight, the Hofmeister effect (the salt-induces attraction) is not sufficient to induce crystallization, as illustrated in figure 2. Here again, the reason why remains unexplained. Fortunately, in such cases polymers like polyethylene glycol (PEG) can do the job as described below.

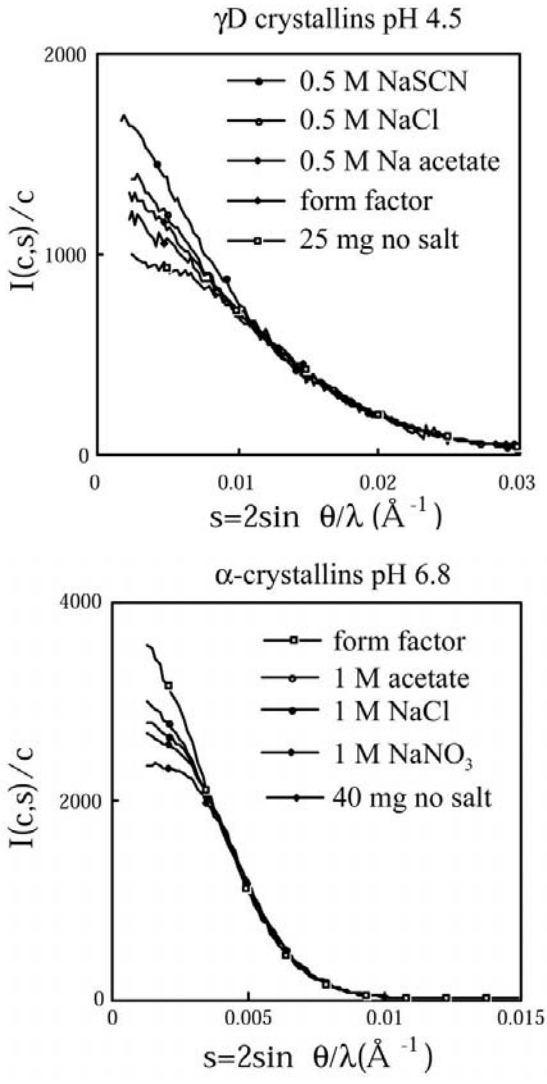

Figure 2
Illustration of the Hofmeister effect. a) The addition of monovalent salt in solutions of small proteins, here the addition of 0.5M salt to 20 kDa gamma-D crystallin solutions, induces an attractive regime : the intensity near the origin is higher than that of the form factor. b) With 800 kDa alpha-crystallins, such a regime is not obtained even at 1M salt. In both cases, a differential effect of anions is observed.

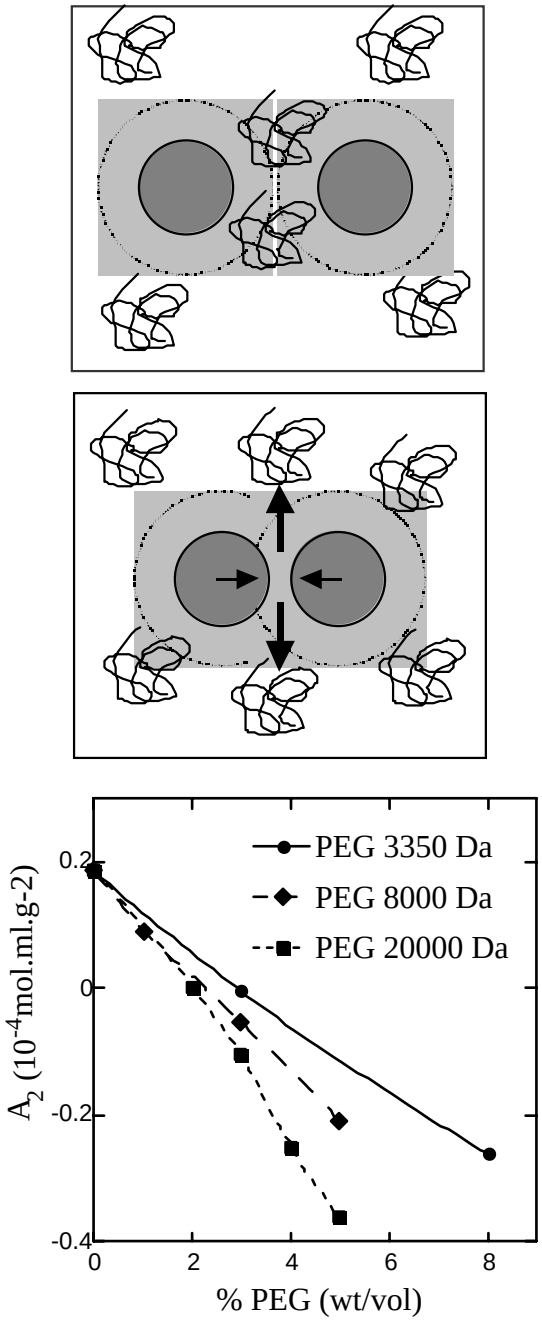

Figure 3
The PEG induced depletion attraction. a) Schematic representation of a PEG-protein mixture, and of the origin of the depletion attraction. b) The attraction induced by the addition of PEGs of various sizes in 128 kDa urate oxidase solutions is sufficient to provide us with negative second virial coefficients (Vivarès & Bonneté, 2002).

3.3. PEG induced crystallization: the depletion attraction

The addition of neutral non-interacting polymers to colloidal solutions is known to induce a depletion attraction (Asakura & Oosawa 1954, Lekkerkerker *et al*., 1992). Similar observations have now been made for protein-PEG mixtures. Because of PEG size and structure, the PEG centers of mass are excluded from the vicinity of the proteins, creating a « depletion zone » as shown in figure 3a.When two neighboring particles get sufficiently close to each other so that their depletion zones overlap, an extra volume is recovered for the polymer thus increasing entropy and lowering the free energy. The phenomenon is therefore equivalent to an effective attraction between the proteins as can be seen on figure 3b (Mahadevan *et al*., 1990, Budayova *et al*., 1999, Hitscherich *et al*., 2000, Kulkarni *et al*., 2000, Bonneté *et al*., 2001, Finet & Tardieu 2001, Vivarès & Bonneté 2002).Only a few PEG-macromolecules phase diagrams have been determined so far, from which the schematic diagram in figure 4a has been established (Odahara *et al*., 1994; Gaucher *et al*.,1997; Casselyn *et al*., 2001). Yet, for a suitable choice of PEG and protein sizes, crystallization is most of the time obtained as shown by the increasing number of PEG grown crystals reported in the literature. As shown in the figure the solubility curve and the solidus curve again delineate the region in between where crystallization can be obtained. As illustrated onfigure 4a a phase separation is usually obtained at sufficiently highPEG and protein concentrations. The phase separation is between one phase enriched in polymer at concentration c_a, and the other in protein at concentration c_b. A variety of microstructures have been observed for the latter**:** fluid, microcrystals or amorphous precipitates (Finet & Tardieu 2001, Casselyn *et al*., 2001).

The study of the interactions showed that, whatever the protein size and charge, the addition of a sufficient amount of PEG of various molecular weights, let say between 0.4 kD and 20kD, induces an attractive regime as illustrated in figure 3b. Eventually, with still increasing attractions, phase separations occur. The effect is mostly independent of temperature. The addition of both PEG and salt do not usually result in the simple addition of the effects of each component taken separately and requires further investigation. The numerical simulation of the depletion attraction induced by PEG is in progress (figure 4b). A major difference with the salt induced attraction is that the depth and range of the attraction may be varied almost at will, simply by changing the polymer size and concentration.

As far as prediction of phase diagrams from interaction forces is concerned, the situation with PEG is at present less advanced than with salt, but much more promising (the point is discussed in Vivarès *et al.*, 2002). The first results indicate that, as for colloids, the phase diagram is essentially a function of the ratio of the radii of gyration of PEG and macromolecule. Since the physics behind is quite well understood, it can be anticipated that we shall be able soon to calculate the size and concentration of PEG to be added in a system to reach the desired attraction and that time and sample consuming experiments will be replaced by much simpler measurements or calculations. Moreover, in practice, the crystallization zone is just below the phase separation zone. The success of PEG to crystallize macromolecules is therefore easily rationalized in terms of depletion attraction.

Since the next challenge in the area probably lies in the understanding of the nucleation process, time-resolved SAXS experiments were undertaken at ESRF to follow the kinetics of PEG-induced phase transitions. Two transitions were investigated, the fluid-fluid phase separation in alpha-crystallin solutions (Finet *et al*., in preparation) and the formation of microcrystals in brome mosaic virus (BMV) solutions, a first account of which is given in this volume (Casselyn *et al*., 2002). One may anticipated that diffracting microcrystals are already visible after 10 seconds.

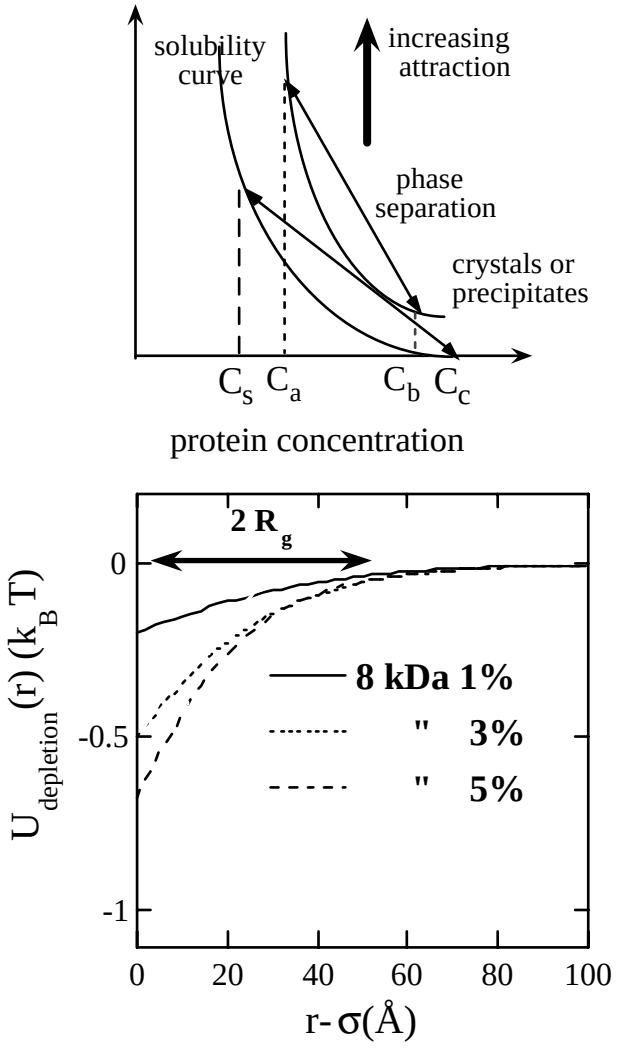

Figure 4
Schematic phase diagram and depletion potential induced by PEG. a) Schematic representation of a typical PEG-protein phase diagram. b) Attractive depletion potentials induced by PEG in urate oxidase solutions (Vivarès *et al*. submitted).

4. Conclusion

The whole of the results obtained indicates that:

- proteins and colloids behave in a similar way;
- the relationship between attractive interactions and crystallization holds whatever the origin of the attraction;
- two types of additives play a central role, salt and PEG; on a theoretical standpoint, the origin of the salt induced attraction is far from clear whereas the PEG-induced depletion attraction is better and better understood.

Moreover, on a practical standpoint, the validity of general rules for biomacromolecular crystallization implies :

- the possibility to rationalize and limit the number of trials for a first screening of crystallization conditions;
- the validity of using the second virial coefficient as a tool to look for crystallization conditions;
- the use of a limited number of crystallizing agents.

Acknowledgments

We gratefully acknowledge the financial support of CNES and CNRS. The experimental work benefited from the efficient support of the technical staff at the synchrotron radiation laboratory LURE-DCI.

References

Arakawa, T. & Timasheff, S. (1985). *Methods in Enzymology*, eds. Wyckoff, H., Hirs, C. & Timasheff, S. N., Vol. 114, pp. 49-77.
Asakura, S. & Oosawa, F. (1954). *J. Chem. Phys.* **22,** 1255-1256.
Atha, D. H. & Ingham, K. C. (1981). *J. Biol. Chem.* **256**, 12108-17.
Belloni, L. (1988). *Chem. Phys.* **88**, 5143.
Bonneté, F., Malfois, M., Finet, S., Tardieu, A., Lafont, S. & Veesler, S. (1997). *Acta Cryst.* D**53**, 438-447.
Bonneté, F., Finet, S. & Tardieu, A. (1999). *J. Crystal Growth*, **196**, 403-414.
Bonneté, F., Vivares, D., Robert, C. & Colloc'h, N. (2001). *J. Crystal Growth*, **232**, 330-339.
Bonneté, F. & Vivares, D. (2002). *Acta Cryst*. D**58**, 1571-1575.
Boyer, M., Roy, M. O., Jullien, M., F., B. & Tardieu, A. (1999). *J. Crystal Growth*, **196**, 185-192.
Budayova, M., Bonneté, F., Tardieu, A. & Vachette, P. (1999). *J. Crystal Growth*, **196,** 210-219.
Carbonnaux, C., Ries-Kautt, M. & Ducruix, A. (1995). *Protein Sci*. **4**, 2123-2128.
Casselyn, M., Pérez, J., Tardieu, A., Vachette, P., Witz, J. & Delacroix, H. (2001). *Acta Cryst.* D**57**, 1799-1812
Casselyn, M., Tardieu, A., Finet, S. & Delacroix, H. (2002). *Acta Cryst.* D**58**, 1568-1570.
Costenaro, L., Zaccai, G. & Ebel, C. (2001). *J. Crystal Growth*, **232**, 102-113**.**
Ducruix, A., Guilloteau, J. P., Riès-Kautt, M. & Tardieu, A. (1996). *J. Crystal Growth*, **168**, 28-39.
Finet, S. & Tardieu, A. (2001). *J. Crystal Growth*, **232**, 40-49.
Finet, S., Narayanan, T. & Tardieu, A. (2002). In preparation.
Gaucher, J.F., Ries-Kautt, M., Reiss-Husson, F. & Ducruix, A (1997). *FEBS Lett.* **401**, 113-116.
George, A. & Wilson, W. W. (1994). *Acta Cryst.* D**50**, 361-365.
Haas, C., Drenth, J. & Wilson, W. W. (1999). *J. Phys. Chem. B,* **103**, 2808-2811.
Hansen, J. P. & Mc Donald, I. R. (1986). *Theory of simple liquids*. 2nd edition, Academic Press, London, Orlando.
Hitscherich, C. J., Kaplan, J., Allaman, M., Wiencek, J. & Loll, P. J. (2000). *Protein Sci*. **9**, 1559-1566.
Hofmeister, F. (1888). *Arch. Exp. Pathol. Pharmakol.* **24**, 247-260.
Kulkarni, A. M., Chatterjee, A. P., Schweizer, K. S. & Zukoski, C. F. (2000.) *J.Chem.Phys*. **113**, 9863-9873.
Lekkerkerker, H. N. W., Poon, W. C. K., Pusey, P. N., Stroobants, A. & Warren, P. B. (1992). *Europhys. Lett.* **20**, 559-564.
Lomakin, A., Asherie, N. & Benedek, G. B. (1996). *J. Chem. Phys.* **104**, 1646-1656.
Mahadevan, H. & Hall, C. K. (1990). *AIChE J.* **36**, 1517-1528.
Malfois, M., Bonneté, F., Belloni, L. & Tardieu, A. (1996). *J. Chem. Phys.* **105**, 3290-3300.
Muschol, M. & Rosenberger, F. (1995). *J. Chem. Phys.* **103**, 10424-10432.
Odahara, T., Ataka, M., & Katsura, M. (1994). *Acta Cryst.* D**50**, 639-642.
Petsev, D. N. & Vekilov, P. G. (2000). *Phys. Rev. Lett.* **84**, 1339-1342.
Riès-Kautt, M. & Ducruix, A. (1989). *J. Biol. Chem.* **264**, 745-748.
Tardieu, A., Le Verge, A., Riès-Kautt, M., Malfois, M., Bonneté, F., Finet, S. & Belloni, L. (1999). *J. Crystal Growth*, **196**, 193-203.
Tardieu, A., Finet, S. & Bonneté, F. (2001). *J. Crystal Growth*, **232**, 1-9.
Velev, O. D., Kaler, E. W. & Lenhoff, A. M. (1998). *Biophys. J.* **75**, 2682-2697.
Vérétout, F., Delaye, M. & Tardieu, A. (1989). *J. Mol. Biol.* **205**, 713-728.
Verwey, E. J. W. & Overbeek, J. T. G. (1948). *Theory of the stability of lyophobic colloïds.*
Vivarès, D. & Bonneté, F. (2002). *Acta Cryst.* D**58**, 472-479.
Vivarès, D., Bonneté, F., Tardieu, A. & Belloni, L. (2002). Submitted.
Vliegenthart, G. A. & Lekkerkerker, H. N. W. (2000). *J. Chem. Phys.* **112,** 5364-5369.
Yau, S. T., Petsev, D. N., Thomas, B. R. & Vekilov, P. G. (2000). *J. Mol. Biol.* **303**, 667-678**.**

 Received 15 April 2002 • Accepted 7 August 2002